



**HAL**  
open science

## Wideband Vector Antenna for Dual-Polarized and 3-D Direction Finding Applications

Johan Duploux, Christophe Morlaas, Hervé Aubert, Patrick Potier, Philippe  
Pouliguen

► **To cite this version:**

Johan Duploux, Christophe Morlaas, Hervé Aubert, Patrick Potier, Philippe Pouliguen. Wideband Vector Antenna for Dual-Polarized and 3-D Direction Finding Applications. *IEEE Antennas and Wireless Propagation Letters*, 2019, 18 (8), pp.1572 - 1575. 10.1109/LAWP.2019.2923531 . hal-02160936

**HAL Id: hal-02160936**

**<https://enac.hal.science/hal-02160936>**

Submitted on 20 Jun 2019

**HAL** is a multi-disciplinary open access archive for the deposit and dissemination of scientific research documents, whether they are published or not. The documents may come from teaching and research institutions in France or abroad, or from public or private research centers.

L'archive ouverte pluridisciplinaire **HAL**, est destinée au dépôt et à la diffusion de documents scientifiques de niveau recherche, publiés ou non, émanant des établissements d'enseignement et de recherche français ou étrangers, des laboratoires publics ou privés.

# Wideband Vector Antenna for Dual-Polarized and 3-D Direction Finding Applications

Johan Duploux<sup>\*†</sup>, Christophe Morlaas<sup>\*</sup>, Hervé Aubert<sup>†</sup>, *Senior Member, IEEE*, Patrick Potier<sup>‡</sup>, and Philippe Pouliguen<sup>‡</sup>

**Abstract**—A wideband and radiation pattern reconfigurable vector antenna is proposed for dual-polarized and 3-D direction finding applications. Compared with the state of the art, this antenna achieves the accurate estimation of the direction of arrival of an incoming vertically- or horizontally-polarized electromagnetic field over a wider bandwidth (7:1). Measurement results are in good agreement with the simulated results obtained from full-wave electromagnetic simulations.

**Index Terms**—wideband magnetic and electric dipoles, Vivaldi antennas, vector sensor, direction-of-arrival antenna, dual-polarized antenna, reconfigurable antenna.

## I. INTRODUCTION

**D**IRECTION Finding (DF) of incoming ElectroMagnetic (EM) fields has become very appealing in many civil and military applications related to radio-navigation or radio-localization [1]. Most of the DF antennas operate over a wide frequency band and estimate the Direction-of-Arrival (DoA) of an incoming EM field over a 2-D angular coverage (i.e., only the azimuth angle is estimated for a restricted range of elevation angles). The DoA estimation relies usually on the spatial diversity of the antenna array [2]. However, there are applications that may require a 3-D angular coverage (i.e., estimation of both azimuth and elevation angles). This coverage can be achieved regardless of the polarization of the incident EM field through an innovative DF technique provided by a Vector Antenna (VA) [3]. Ideally, the VA enables the measurement of the six components of the incoming EM field (i.e.,  $E_x$ ,  $E_y$ ,  $E_z$ ,  $H_x$ ,  $H_y$  and  $H_z$  in the Cartesian coordinate system), allowing the DoA estimation across the 3-D space.

Many VAs have been reported over the last few years, including the active solution covering frequencies below 30 MHz [4] and the passive and dual-band solution operating at GSM frequencies [5]. Very recently, the authors proposed the first passive, wideband and radiation pattern (RP) reconfigurable VA [6]–[8], referred here to as the *Two Season* VA. The measured electrical characteristics of this antenna are detailed in [6], while its simulated and

measured DF performances are reported in [7] and [8], respectively. As in [5], the *Two Season* VA is only able to estimate the DoA of vertically-polarized EM fields, since only three components can be measured ( $E_z$ ,  $H_x$ , and  $H_y$ ). The *Two Season* VA enables the accurate DoA estimation over a measured impedance bandwidth of 1.69:1 (or [2.10 GHz - 3.55 GHz]).

In this letter, a novel VA, referred here to as the *Four Season* VA, is proposed. Compared to the previous 4-port *Two Season* VA, this new VA enables the DoA estimation of an incoming EM field, whatever its polarization and over a wider bandwidth (7:1, or [1 GHz - 7 GHz]). These improved DF performances resulted from: (i) the modification of the VA feeding circuit, and (ii) the addition of the horizontal EM sensor. Moreover, despite the more complex feeding circuit (eight ports), it is shown that the accuracy of the DoA estimation of an incident vertically-polarized EM field is improved thanks to the measurement of the horizontal components ( $E_x$ ,  $E_y$  and  $H_z$ ).

## II. THE *Four Season* VECTOR ANTENNA

### A. Design consideration

The *Four Season* VA consists of the *Two Season* VA (vertical part of the VA depicted in Fig. 1(a)) mounted over a 4-port circular array of eight Vivaldi antennas (see details in Fig. 1(c&d) and Table I). Compared with the *Two Season* VA, the *Four Season* VA is intended to estimate the DoA of incident horizontally-polarized EM fields in order to reduce the estimation errors due to polarization mismatch. This antenna allows the measurement of six EM field components. The idea is to replace the metallic support of the *Two Season* VA by eight additional radiating elements feeded through four ports. These elements serve as a ground plane for the two vertical semi-circular arrays and as an EM sensor for measuring the three components  $H_z$ ,  $E_x$  and  $E_y$  (that could not be measured in [8]). More specifically, the horizontal circular array is the 1.5 scale-up replica of the semi-circular arrays of the *Two Season* VA. Moreover, the power splitter part of the feeding circuit of the Vivaldi antennas has been modified. Contrary to what is stated in [6], the input impedance of the Vivaldi antennas is about 100  $\Omega$  (and not 65  $\Omega$ ) when antennas are connected within the array. Therefore, the 1:2 microstrip line power splitter used in [6], and fabricated using the T-junction and impedance transition lines (Fig. 1(f)), can be advantageously replaced by two 100  $\Omega$  parallel microstrip

<sup>\*</sup> Ecole Nationale de l'Aviation Civile, Université de Toulouse, F-31055 Toulouse, France (e-mail: christophe.morlaas@enac.fr).

<sup>†</sup> LAAS-CNRS, Micro and Nanosystems for Wireless Communications Research Group, F-31055 Toulouse, France, and the National Polytechnic Institute, F-31055 Toulouse, France.

<sup>‡</sup> Direction Général de l'Armement (DGA), F-75509 Paris, France.

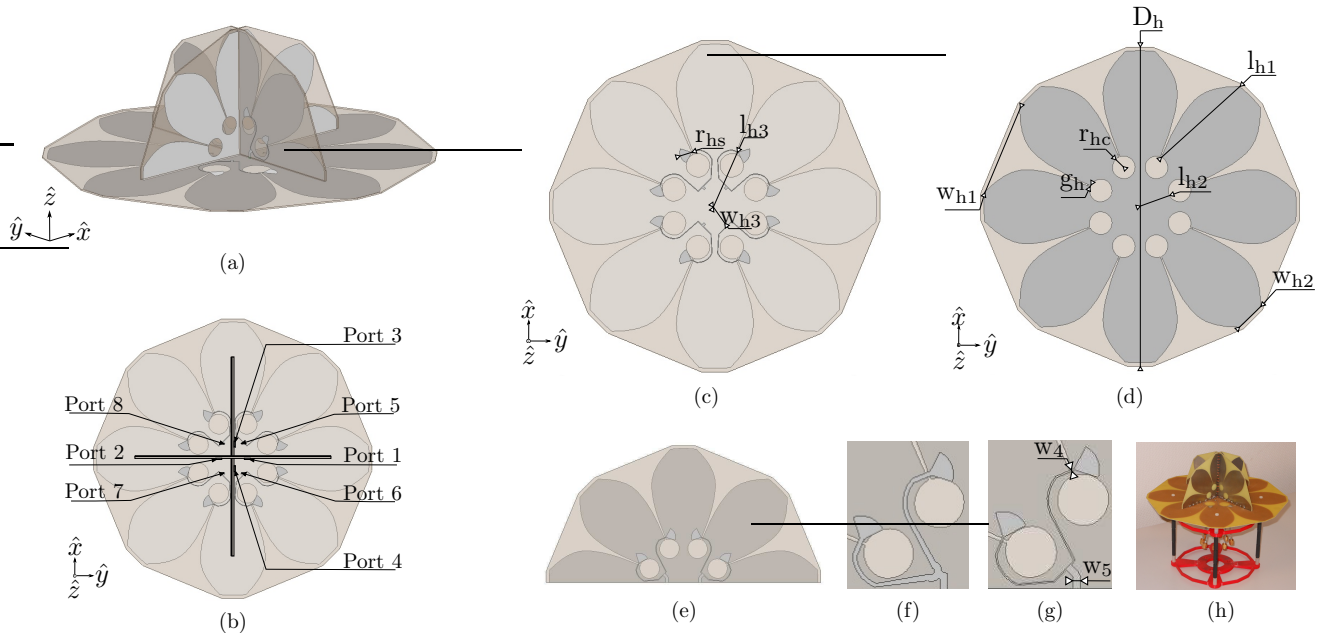


Fig. 1. Geometry (a), ports numbering (b), and fabricated prototype (h) of the *Four Season* VA. Top (c) and back (d) views of the horizontal part constituting the VA. Geometry of the vertical arrays of the VA (e) with a zoom on the previous (f) and new (g) feeding circuits.

lines connected to the  $50 \Omega$  input port (Fig. 1(g)). Hence, compared with [6], the new dimensions of the VA feeding circuit (reported in Table I) allows the significant enlargement of the impedance bandwidth (see Section III-A).

TABLE I  
DIMENSIONS OF THE HORIZONTAL CIRCULAR ARRAY

Parameter	$D_h$	$l_{h1}$	$l_{h2}$	$l_{h3}$	$W_{h1}$	$W_{h2}$
Value (in mm)	230	75.75	22.5	40.6	65.7	21.6
Parameter	$W_{h3}$	$g_h$	$r_{hc}$	$r_{hs}$	$W_4$	$W_5$
Value (in mm)	13.9	0.9	8.25	8.25	0.36	1.58

### B. Signal processing consideration

Following [6], the measurement of the EM field components  $H_x$ ,  $H_y$  and  $E_z$  are performed from three sets of weighting coefficients assigned to the received signals at the VA vertical ports (denoted by the acronym RPC 0, which stands for Radiation Patterns Combination 0). According to the mirror symmetry between the two feeding circuits of the 2-port vertical array (Fig. 1(e)) along the  $y$ -axis (resp.  $x$ -axis), the component  $H_x$  (resp.,  $H_y$ ) can be measured when ports 1 and 2 (resp., ports 3 and 4) are out of phase (i.e., by applying the weighting coefficients  $[1,-1]$ ) in order to excite in phase the four Vivaldi antennas to form a magnetic dipole. The component  $E_z$  is measured by recombining all the ports of the vertical part of the VA in phase  $[1,1,1,1]$  to form an electric dipole oriented along the  $z$ -axis. The other three components  $H_z$ ,  $E_x$  and  $E_y$  can also be derived from three additional sets of weighting coefficients assigned to the received signals at the VA horizontal ports. Again, according to the mirror symmetry between the feed structures of two adjacent Vivaldi antennas (Fig. 1(c)), the component  $H_z$  can be measured if the eight Vivaldi antennas of the horizontal array are

in-phase fed to operate as a magnetic dipole, which can be achieved by applying  $[1,-1,1,-1]$  on ports 5 to 8. The component  $E_x$  (resp.,  $E_y$ ) is measured by recombining the ports of the VA horizontal part  $([1,-1,-1,1], \text{ resp. } [1,1,-1,-1])$  in order to create a magnetic wall along the  $xz$ -plane (resp.  $yz$ -plane) and an electric-wall along the  $yz$ -plane (resp.  $xz$ -plane) to form an electric dipole oriented along the  $x$ -axis (resp.,  $y$ -axis). The weighting coefficients associated with the measurement of the six EM field components are summarized in Table II (RPC 00).

TABLE II  
SET OF WEIGHTING COEFFICIENTS ASSIGNED TO THE SIGNALS RECEIVED AT THE EIGHT PORTS OF THE *Four Season* VA FOR MEASURING THE SIX COMPONENTS OF AN INCOMING EM FIELD

Measured Component	Port							
	1	2	3	4	5	6	7	8
RPC 00	$H_x$	1	-1	0	0	0	0	0
	$H_y$	0	0	1	-1	0	0	0
	$E_z$	1	1	1	1	0	0	0
	$H_z$	0	0	0	0	1	-1	1
	$E_x$	0	0	0	0	1	-1	-1
	$E_y$	0	0	0	0	1	1	-1

### III. SIMULATED AND MEASURED ELECTRICAL PERFORMANCES

The electrical performances (impedance matching and radiation patterns) of the *Four Season* VA have been assessed using full-wave EM simulations (Ansys HFSS) and from measurements carried out in an anechoic chamber. A photograph of the prototype is given in Fig. 1(h).

#### A. Impedance matching and mutual coupling

The VSWR of the *Four Season* VA is shown in Fig. 2. The measured impedance bandwidth of the vertical and

horizontal radiating elements is of 6.77:1 (or [1.24 GHz - 8.40 GHz]) and 10.74:1 (or [0.79 GHz - 8.49 GHz]) for a  $VSWR \leq 2.3$ , respectively. As the horizontal circular array is the scale-up replica of the semi-circular array of the *Two Season* VA, there is approximately a factor 1.5 between the lower operating frequency of the vertical and horizontal radiating elements. Moreover, there is a good agreement between simulation and measurement results, even if the measured  $VSWR$  at the vertical ports is slightly degraded at high frequencies due to technological inaccuracies in the prototype manufacturing process. Hence, the impedance bandwidth of the prototype is limited to 6.77:1 (or [1.24 GHz - 8.40 GHz]). The *Four Season* VA is included within a half-sphere of radius  $0.47\lambda_{1.24\text{GHz}}$ . Besides, the radius of the horizontal circular array is  $0.30\lambda_{0.79\text{GHz}}$ , while the radius of the vertical semi-circular arrays is of  $0.32\lambda_{1.24\text{GHz}}$ . This corresponds approximately to a reduction by a factor 1.6 of the electrical size of the vertical part of the *Two Season* VA.

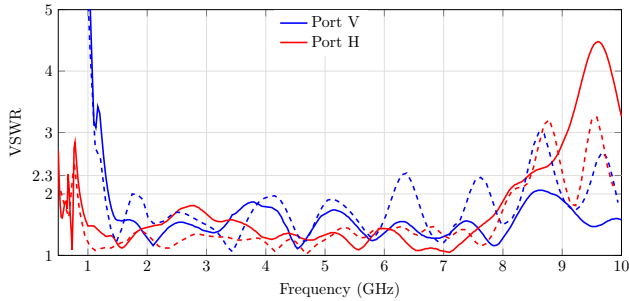


Fig. 2. Simulated (solid line) and measured (dashed line)  $VSWR$  of the *Four Season* VA as a function of frequency. For symmetry reasons, only measurement at one vertical (V) port and one horizontal (H) port are plotted.

The measured isolation between the ports of the *Four Season* VA is depicted in Fig. 3. It can be observed that the mutual coupling between the vertical ports (ports  $i \in [1, 4]$ ) does not exceed -10 dB across the overall bandwidth and even -20 dB from 1.8 GHz. As for the vertical ports (ports  $i \in [5, 8]$ ), it is less than -20 dB in the operating frequency range. The same level of isolation is achieved between the vertical and horizontal ports.

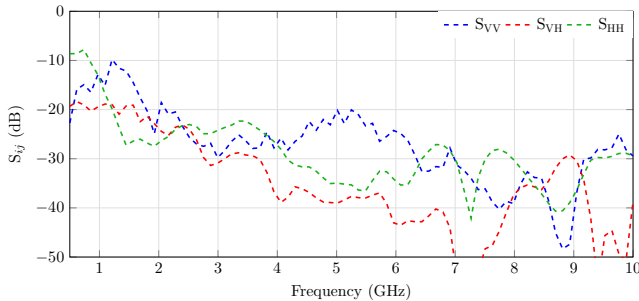


Fig. 3. Measured isolation between the vertical (V) or/and horizontal (H) ports of the *Four Season* VA as a function of frequency. Only the highest (i.e., worst-case) mutual couplings  $S_{ij}$  are plotted.

## B. Radiation patterns

The RPs of the *Four Season* VA associated with the measurement of the six components of an incoming EM field are depicted in Fig. 4. For symmetry reasons, the RPs associated with the measurement of  $E_y$  and  $H_y$  are not shown here. It can be observed that the RPs are similar to those of electric and magnetic dipoles in their respective E-plane and H-plane. As expected from Chu's theory [9], some ripples appear in the RPs of the electric and magnetic dipoles as the frequency increases. However, there is an overall good agreement between the measured and the simulated RPs. Moreover, for some frequencies, the size of the horizontal antenna elements impacts the RP of the vertical antenna elements. For example, at 5 GHz in Fig. 4(g), the radiation level is reduced in the y-axis direction and more sidelobes appear. However, this RP modification does not impact the DOA estimation performance.

## IV. SIMULATED AND MEASURED DIRECTION FINDING PERFORMANCES

The DF performances of the *Four Season* VA have been evaluated in the 3-D upper half space using the MUSIC algorithm [10] and from full-wave EM simulation or measurement data. The accuracy of the DoA estimation is evaluated through the angular error  $\Delta a_{RMS}$  between the estimated angles of arrival and the exact angles (see, e.g., Eq. (9) in the Appendix of [8] for the detailed definition), and its 95<sup>th</sup> percentile, which indicates the maximum error for 95% of all estimated DoAs. The estimation parameters are those given in [8], except that the DoA estimation is performed using the six components (instead of the three components) of the incoming EM field (RPC 00) from 1 GHz to 8.2 GHz with a 0.4 GHz frequency step. This incoming EM field is either vertically- or horizontally-polarized. Moreover, as described in [5], the calibration matrix derived from the simulated or measured RPs of the antenna is used for taking into account the eventual amplitude and phase distortions. Fig. 5 displays the 95<sup>th</sup> percentile of  $\Delta a_{RMS}$  for an incoming vertically- or horizontally-polarized EM field. For comparison purpose, the DoA estimation accuracy of a vertically-polarized incident EM field obtained from using only RPC 0 (that is, from only the measurement of the three field components  $H_x$ ,  $H_y$  and  $E_z$ ) is also depicted. It can be observed that the additional measurement of the field components  $E_x$ ,  $E_y$  and  $H_z$  improves the DoA estimation of the vertically-polarized EM field in terms of accuracy and frequency coverage. The measured 95<sup>th</sup> percentile of  $\Delta a_{RMS}$  does actually not exceed 5° from 1 GHz up to approximately 7.0 GHz. Moreover, the DoA estimation of the horizontally-polarized EM field is also very accurate, since the measured 95<sup>th</sup> percentile of  $\Delta a_{RMS}$  is smaller than 2° up to 8.2 GHz. In addition, there is a good agreement obtained between the simulated and measured results. Fig. 6 displays the measured angular distance  $\Delta a_{RMS}$  achieved from the *Four Season* VA at the central frequency (3.8 GHz) using

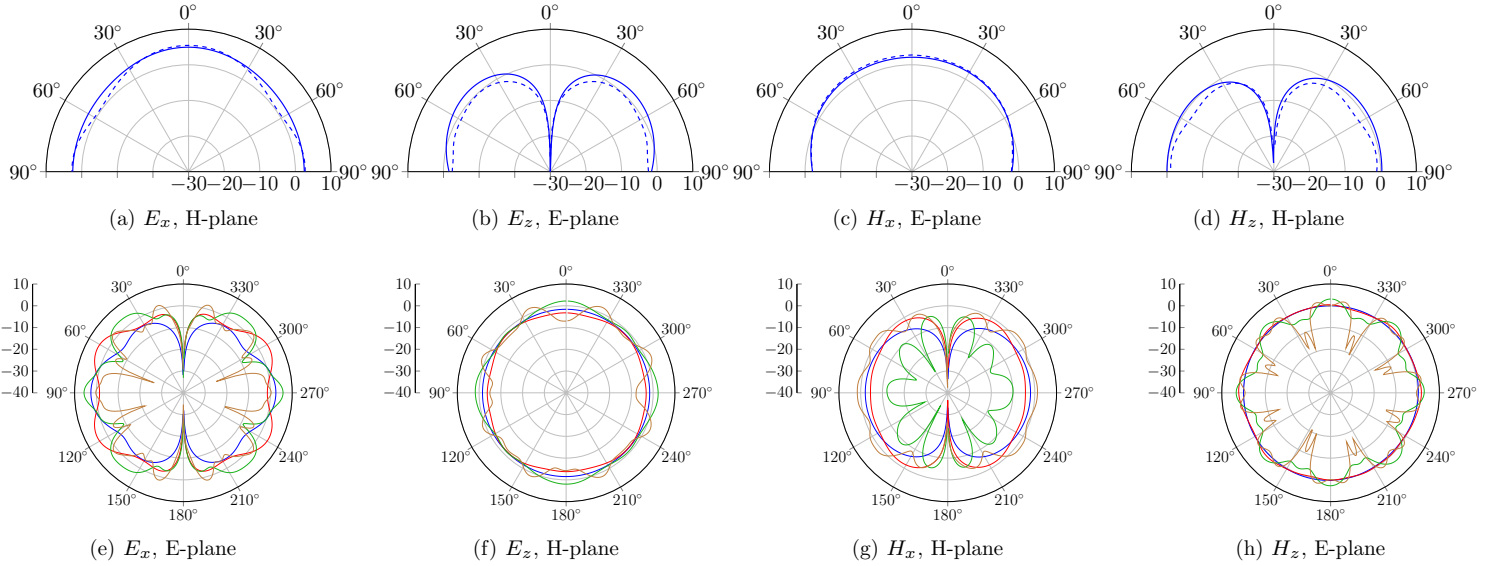


Fig. 4. Simulated (solid line) and measured (dashed line) realized gain of the *Four Season* VA in  $\theta$ -polarization (columns 2 and 3) and  $\phi$ -polarization (columns 1 and 4) associated with the sets of weighting coefficients assigned to the eight input ports of the antenna (specified in Table II) for measuring the component: (a) & (e)  $E_x$ , (b) & (f)  $E_z$ , (c) & (g)  $H_x$ , (d) & (h)  $H_z$  at 1.4 GHz (blue line), 2.8 GHz (red line), 5 GHz (green line) and 8 GHz (brown line). The top and bottom figures correspond to the RPs in the  $\hat{y}\hat{z}$ -plane and  $\hat{x}\hat{y}$ -plane, respectively.

RPC 0 or RPC 00 in the DoA estimation process. It can be observed that using RPC 00 instead of RPC 0 enhances the accuracy of the DoA estimation of the vertically-polarized EM field in the angular area in which the estimation errors were maximum. Furthermore, the  $\Delta a_{\text{RMS}}$  does not exceed  $5^\circ$  in every direction of the 3-D upper half space for both polarizations of the incoming EM field when RPC 00 is used. Finally, these results confirm that the *Four Season* VA can be used for dual-polarized and 3-D DF applications with a very good DoA estimation accuracy over a 7:1 bandwidth (or [1 GHz - 7 GHz]).

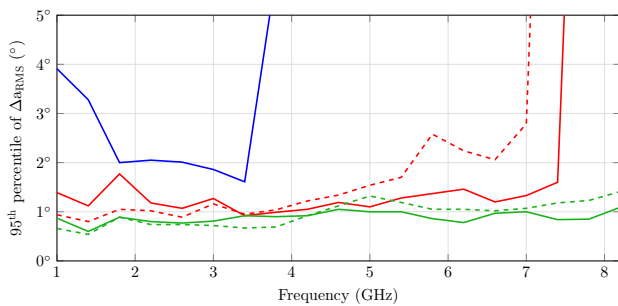


Fig. 5. Simulated (solid line) and measured (dashed line) 95<sup>th</sup> percentile of  $\Delta a_{\text{RMS}}$  obtained from the *Four Season* VA for the estimation of the: (a) vertically- (red line) or (b) horizontally-polarized (green line) EM field using RPC 00. The blue line corresponds to the DoA estimation accuracy of the vertically-polarized EM field achieved from RPC 0.

## V. CONCLUSION

A wideband VA for dual-polarized and 3-D DF application has been presented in this letter. The measurement of the six components of the vertically- or horizontally-polarized incoming EM field is performed from the RP

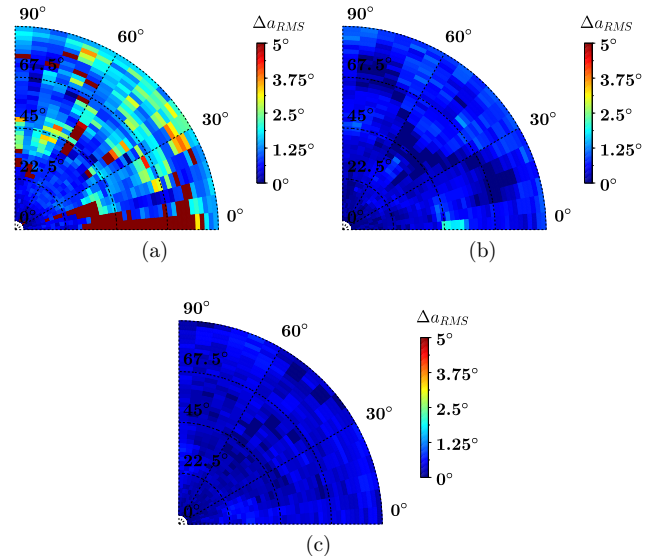


Fig. 6. Measured  $\Delta a_{\text{RMS}}$  at 3.8 GHz obtained from the *Four Season* VA using (a) RPC 0 or (b&c) RPC 00 for the estimation of the: (a&b) vertically- or (c) horizontally-polarized EM field.

reconfigurability of two orthogonal and colocated semi-circular arrays mounted over a circular array of Vivaldi antennas. Such VA enables the accurate estimation of the DoA across the 3-D upper half space and over a wide bandwidth (7:1). The measurement results have confirmed the simulated performances. Future works will be focused on improving the DF performances of this VA in electromagnetic reverberant and/or multi-source environments, and reducing the antenna size.

## ACKNOWLEDGMENT

The authors acknowledge the French Defense Agency (Direction Général de l'Armement, DGA) and the Occitanie regional council for their financial support.

## REFERENCES

- [1] T. E. Tuncer and B. Friedlander, *Classical and Modern Direction-of-Arrival Estimation*. Academic Press, 2009.
- [2] P. Gething, *Radio Direction Finding and Superresolution*, ser. Electromagnetics and Radar. P. Peregrinus Ltd., 1991.
- [3] A. Nehorai and E. Paldi, "Vector-sensor array processing for electromagnetic source localization," *IEEE Transactions on Signal Processing*, vol. 42, no. 2, pp. 376–398, Feb. 1994.
- [4] B. Almog, "Compact 3D direction finder," Patent EP20 120 184 835, 2013.
- [5] J. Lominé, C. Morlaas, C. Imbert, and H. Aubert, "Dual-band vector sensor for direction of arrival estimation of incoming electromagnetic waves," *IEEE Transactions on Antennas and Propagation*, vol. 63, no. 8, pp. 3662–3671, Aug. 2015.
- [6] J. Duploup, C. Morlaas, H. Aubert, P. Potier, P. Pouliguen, and C. Djoma, "Reconfigurable grounded vector antenna for 3-D electromagnetic direction-finding applications," *IEEE Antennas and Wireless Propagation Letters*, vol. 17, no. 2, pp. 197–200, Feb 2018.
- [7] —, "3D direction-of-arrival estimation using a wideband vector antenna," in *IEEE International Symposium on Antennas and Propagation (APSURSI)*, Boston, July 2018.
- [8] J. Duploup, C. Morlaas, H. Aubert, P. Potier, and P. Pouliguen, "Wideband and reconfigurable vector antenna using radiation pattern diversity for 3-D direction-of-arrival estimation," *IEEE Transactions on Antennas and Propagation*, in press.
- [9] T. S. Chu, "On the use of uniform circular arrays to obtain omnidirectional patterns," *IRE Transactions on Antennas and Propagation*, vol. 7, no. 4, pp. 436–438, October 1959.
- [10] R. Schmidt, "Multiple emitter location and signal parameter estimation," *IEEE Transactions on Antennas and Propagation*, vol. 34, no. 3, pp. 276–280, Mar. 1986.